J Solid State Electrochem (1999) 3: 457–463

ORIGINAL PAPER

A.N. Kamkin · Guo-Ding Zhou · A.D. Davydov

Photoelectrochemical characteristics of oxide layers on copper-nickel alloys

Received: 15 June 1998 / Accepted: 16 November 1998

Abstract The electrochemical behavior of a series of Cu-(7, 30, 50, 70 wt%)Ni alloys in borate buffer and sodium sulfate solutions with and without argon purging was studied by cyclic voltammetry and the photocurrent response method. It is shown that nickel has an effect on both the dark and photocurrents and stimulates oxide film formation. The measurements show that oxygen leads to the formation of passivating p-type Cu_2O layers. In sulfate solution this type changes at the potential of the onset of intense alloy dissolution.

Introduction

Oxide films (OF), which are formed on alloy surfaces, have a pronounced effect on the electrochemical properties and corrosion of the alloys. At present, only a few methods are available which make it possible to study the OF *in situ* in solution. The photoelectrochemical method, which enables the characteristics of semiconductive OF to be determined, is among these methods. This method may serve as a significant supplement to the traditional electrochemical methods for investigating the electrochemical behavior of alloys.

A considerable number of photoelectrochemical studies have been performed on OF on many pure metals, while the OF on alloys have received much less attention. Studies of OF on pure copper using cyclic voltammetry (CV) [1, 2] and the photoelectrochemical method [3–6] have shown that the presence of Cu_2O, CuO, and CuO + $Cu(OH)_2$ on the copper surface may be found, depending on the electrode potential and solution composition. The CV curves exhibit the characteristic peaks corresponding to the regions of metal oxidation and oxide reduction. Cu_2O is a semiconductor with a band gap of about 3.2 eV [3–6] and is suitable for photoelectrochemical studies: it is readily detected in the region of visual light. CuO is not detectable by the photoelectrochemical method because of its very low band gap (about 0.5–0.6 eV).

It was shown for nickel that the semiconductive oxide NiO with a band gap of 3.4 eV is the main oxide grown in most solutions [7–9]. In [9], the photocurrents were measured at −0.2 V for nickel with the OF formed at +0.8 V (NHE) in a borate buffer solution.

So far, only a few systematic electrochemical investigations have been conducted on Cu-Ni alloys [10–13]. Many papers concern the composition of surface oxides on each alloy as studied by *ex situ* physical methods [14–19]. For example, for Cu10Ni and Cu30Ni it has been shown [16, 17] that both copper and nickel are present in the film of the corrosion products. A detailed investigation of the oxide films which formed on different Cu-Ni alloys, as a function of potential, was conducted by Strehblow and co-workers [18, 19] and a two-layer model for such film formation was proposed.

Studies using the *in situ* method of differential reflectometry [20, 21] demonstrated the simultaneous presence of Cu_2O and NiO on the surface of the alloy Cu70Ni.

No photoelectrochemical studies of the entire series of Cu-Ni alloys are available. However, it was shown [22] by examing the photopotentials for Cu-Ni alloys in 0.1 M NaCl that there is a correlation between the alloy composition, corrosion rate, and type of surface film conductivity. For pure nickel and Cu70Ni alloy the corrosion rate is low, and the film is a p-type semiconductor. For other alloys (Cu30Ni, Cu10Ni, and Cu) in this solution the corrosion rate is high, and the film is an n-type semiconductor. For copper and Cu30Ni it has been found [23] that the corrosion behavior varies with the type of film conductivity.

A.N. Kamkin
Moscow State University, Vorob'evy Gory, Moscow 119899, Russia

G.-D. Zhou
Shanghai Institute of Electric Power, Shanghai 200090, China

A.D. Davydov
Frumkin Institute of Electrochemistry, Russian Academy of Sciences, Leninskii pr. 31, Moscow 117071, Russia

The aim of the present work was to study the electrochemical behaviour of Cu-Ni alloys using voltammetry while simultaneously recording the photocurrents arising from the specimen illuminated with modulated light.

Experimental

The specimens were made of Cu*X*Ni alloys (where X = 7, 30, 50, and 70 wt%); two solutions, a borate buffer solution (0.15 M H_3BO_3 + 0.075 M $Na_2B_4O_7$, pH 8.7) and a 0.1 M Na_2SO_4 solution (pH 9.1), were used for the study. The alloys were melted in a vacuum furnace from pure copper (99.999) and nickel (99.99). Plates of 8 × 8 × 2 mm size were cut from the ingots produced; the current leads were soldered to one side of the plate. This side and the end-faces of the plate were insulated with epoxy resin. At the working plate side, the alloy composition was determined by X-ray spectral microanalysis. The electrode working surface was abraded with emery paper, polished with aluminum oxide powder of 0.5 μm grade, and rinsed with ethyl alcohol and deionized water.

The potentiodynamic curves were measured with a sweep rate of 2 mV/s; both dark and illuminated situations were studied. The specimens were illuminated with a 500 W Xe lamp through a quartz window in the electrochemical cell, using a focusing lens, a monochromator (spectral gap width of 10 nm), and a mechanical chopper with a frequency of 38 Hz for light modulation in the range of λ from 300 to 700 nm. The luminous flux power did not exceed 20 mW/cm. The experimental set-up involved a PAR-273 potentiostate, a two-coordinate two-channel recorder, and a lock-in analyzer PAR M5208EC.

Immediately prior to each experiment the specimen was cathodically reduced in a special cell in the working solution at 3–4 mA/cm^2 for 25–30 min. The experiment began as soon as the specimen was placed into the main electrochemical cell. In some experiments, to remove the dissolved oxygen the solution in the cell was purged with extra pure argon for 30 min prior to the experiment and then throughout the measurements. The solution was replaced after 3–5 experiments.

For all specimens, the potentiodynamic curves were measured from −1.0 V to +0.8 V (direct scan) and reversed to the potential of the onset of noticeable hydrogen evolution (its value ranged from −0.7 to −0.9 V for various alloys) (reverse scan). All potentials are given with reference to the saturated calomel electrode (SCE).

The previous data and our preliminary experiments with pure nickel have shown that the photocurrents are very low and can be recorded only in the reverse scan of the potentiodynamic curve at λ < 320 nm, after −0.7 to −0.8 V is reached, i.e. slightly before or simultaneously with the onset .

The photocurrents on copper characterizing Cu_2O may be measured during anodic and cathodic cycles of the potentiodynamic curve at λ = 350–550 nm. In this case the photocurrents on copper are 10–100 times higher than those on nickel. Hence, we propose that the photocurrent at the wavelength of 420 nm (3.0 eV) corresponds to Cu_2O in all potentiodynamic experiments on the alloys.

Results and discussion

Deaerated borate buffer solution

Copper

A potentiodynamic curve (positive-going and reverse scans) presenting a dependence of dark current on the potential is shown as a dashed line in the upper part of Fig. 1. The anodic branch (the direct scan) is characterized by the three peaks A1, A2, and A3 corresponding to the formation of Cu_2O (peak A1), dissolution yielding Cu^+ (peak A2)[1] and formation of a CuO and $Cu(OH)_2$ mixture (peak A3) [1, 3, 6, 24].

In the cathodic branch (the reverse scan), two peaks corresponding to reduction are observed: CuO or $Cu(OH)_2 \rightarrow Cu_2O$ (peak C2) and $Cu_2O \rightarrow Cu$ (peak C1).

A comparatively small photocurrent is observed for copper during the anodic scan in the potential region of the anodic peak A1 (the lower part of Fig. 1). The considerable photocurrents which are measured during the reverse scan correspond to the cathodic peak C2, i.e. to the photoactive Cu_2O formation. When the C1 maximum is reached, the photocurrent decays to zero.

Nickel

In the anodic branch of the curve for nickel (dot-and-dash line in the upper part of Fig. 1), one peak corresponding to NiO formation is observed [10, 20]. The cathodic branch with very small currents for passive nickel indicates that oxide reduction does not occur.

No photocurrents were recorded during either the anodic cycle or the cathodic cycle (including at λ = 280–300 nm).

Copper-nickel alloys

Deoxygenated borate buffer solution. The anodic behavior of alloys (Fig. 1) is as follows: addition of nickel to copper leads first to an increase of the peak A1 (Cu7Ni and Cu30Ni alloys) and, then, to its decrease (Fig. 2). The anodic peak, which is typical of pure nickel, is present only for alloys rich in nickel (Cu70Ni) as a slight increase of current before peak A1 in the potential range from −0.5 to −0.05 V.

Thus, nickel, which is less prone to passivity in the potential range studied, causes a not quite clear increase in the anodic current for the alloys in which the nickel content does not exceed 50%. As expected, alloys with a higher Ni content exhibit passivity. It should be noted that the passivating properties of Ni are observed for alloys with copper, if its concentration is 50 wt% and higher [10–13].

[1] In alkaline solutions the second peak is usually related to the formation of CuO [1, 2, 6]. However, in borate buffer solution, copper dissolution yielding Cu^{2+} occurs in the second peak region [24]. In our experiments the second peak lies 50–70 mV more negative than the peak of CuO formation. Because of that and because the anodic peak for Cu reappeared on reverse scan at these potentials, we propose that it was due to Cu dissolution as Cu^+ ions.

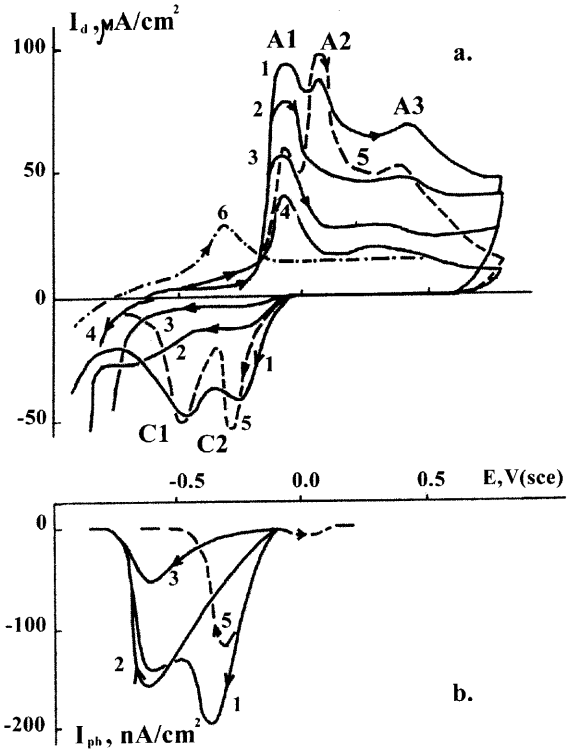

Fig. 1 a Dependence of dark current i_d and **b** corresponding dependence of photocurrent i_{ph} (λ = 420 nm) on the potential in the deaerated borate buffer solution. Hereafter, the numbers denote: *1* Cu7Ni, *2* Cu30Ni, *3* Cu50Ni, *4* Cu70Ni, *5* Cu, *6* Ni. Direction of the potential scan (2 mV/s) is shown by an *arrow*

The peak A2 is observed only in the curve of the Cu7Ni alloy. Higher nickel amounts lead to its disappearance, i.e. nickel inhibits the dissolution.

The current of peak A3 is higher in the curve of the Cu7Ni alloy than in the curve for copper, but it decreases with an increase in the nickel content, i.e. an activating effect of nickel on the alloy manifests itself in a narrower range of Ni content in the peak A3 than in the peak A1.

The cathodic branch of the CVs of the alloys shows that introduction of 7% nickel into the alloy leads to insignificant changes of the maximum currents in the peaks C2 and C1 in relation to copper, but to a marked increase in the peak areas (i.e. in the amount of nickel oxide reduced).

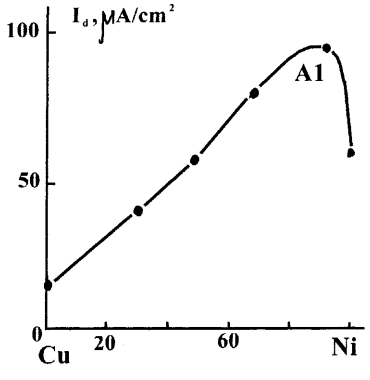

Fig. 2 Dependences of currents of peak A1 on the Cu-Ni alloy composition for borate buffer solution (potential scan rate 2 mV/s)

Large amounts of nickel in the alloy cause a decrease in both peaks up to their total disappearance for the alloy Cu70Ni; for this alloy, the cathodic curve almost coincides with the curve for pure nickel. The charge of the anodic cycle is larger than that of the cathodic cycle; the relation between anodic and cathodic charges which characterizes the irreversibility of the process increases with the increase of the nickel content. Probably this indicates, first, that a fraction of the anodic current is used for alloy dissolution; the smaller the nickel content of the alloy, the larger is this part. Second, the oxide reduction is hampered (during the cathodic cycle). The currents are higher for the Cu7Ni alloy than for copper, i.e., in this case, probably, nickel promotes alloy dissolution.

The photocurrent measurements yielded the following results: no photocurrent was detected during the anodic scan for the alloys as opposed to pure copper. For pure copper, the photocurrent was recorded in the region of peak A1 and corresponded to Cu_2O formation. However, after the alloy specimens were held at the peak A1 potentials for 20 min, a small photocurrent arose. The smaller the nickel content, the higher the photocurrent was. This points to a possibility of markedly slower Cu_2O formation on the alloys than on pure copper at the potentials of peak A1. Probably, for alloys, on the positive-going scan, the dark current of peak A1 is consumed by dissolution to a greater extent. An increase of this peak in the curves of the Cu7Ni and Cu30Ni alloys relative to the curves for pure copper also suggests that nickel promotes alloy dissolution.

During the reverse scan the photocurrents of the alloys are readily recorded. In the curve for Cu7Ni, two peaks are observed at the potentials which correspond to the dark-current peaks C2 and C1. In the curves of Cu30Ni and Cu50Ni, one peak corresponding to peak C1 is readily seen. No photocurrent is detected for Cu70Ni.

The first photocurrent peak of Cu7Ni, as well as for pure copper, corresponds to the formation of photoactive Cu_2O as a result of CuO reduction. A much higher photocurrent peak of alloy than of copper indicates that a much larger oxide amount has been formed during the positive-going scan on the alloy than on copper.

The second peak (in the region of more negative potentials) in the photocurrent curve of Cu7Ni and the peaks in the photocurrent curves of Cu30Ni and Cu50Ni are, evidently, associated with the presence of nickel in the alloy. However, as noted above, nickel itself does not yield a photocurrent but could save copper oxide during the anodic scan.

Borate buffer solution containing dissolved oxygen. Figure 3 gives the potentiodynamic curves, which are measured for the pure copper and copper-nickel alloys

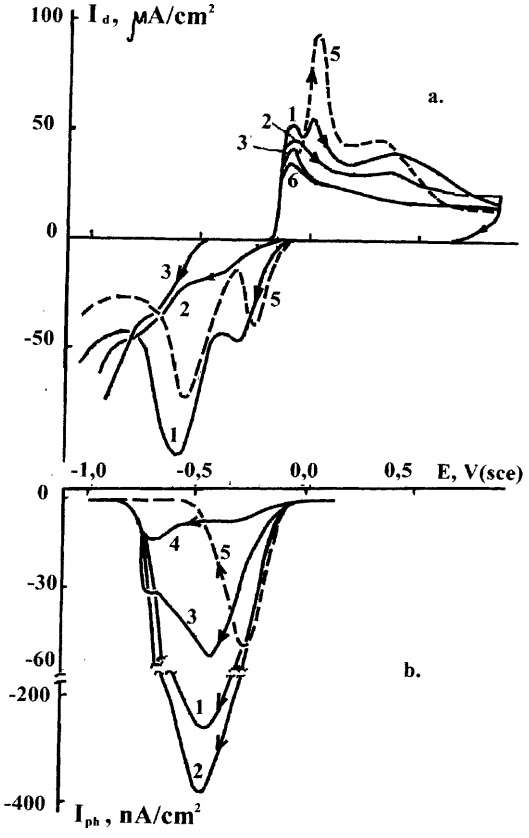

Fig. 3 **a** Dependence of dark current i_d and **b** corresponding dependence of photocurent i_{ph} (λ = 420 nm) on the potential for Cu-Ni alloys in the oxygen containing borate buffer solution (potential scan rate 2 mV/s)

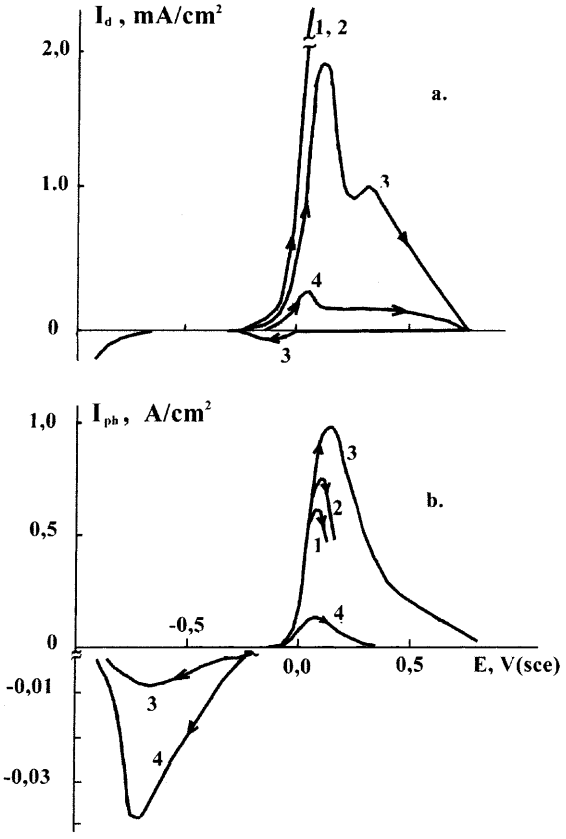

Fig. 4 **a** Dependence of dark current i_d and **b** corresponding dependence of photocurent i_{ph} (λ = 420 nm) on the potential for Cu-Ni alloys in the deaerated Na_2SO_2 solution (potential scan rate 2 mV/s)

in the borate buffer solution; dissolved oxygen has not been removed from the solution. The main differences from the results of the oxygen-free solutions are as follows: the anodic currents of the copper and high copper alloys are significantly lower here. The cathodic currents of copper and Cu7Ni in the region of peak C2 are markedly higher than in the region of peak C1. On the high-nickel alloys the photocurrent is detected essentially earlier: at potentials 150–250 mV more positive than the dark current of oxide reduction. The photocurrents of copper are lower and the photocurrents of Cu7Ni and Cu30Ni are higher than in the deaerated solution.

As would be expected, the presence of dissolved oxygen promotes alloy passivation.

Sodium sulfate solution

Potentiodynamic curves

Figures 4 and 5 give the results of the electrochemical study of the Cu-Ni alloys in a 0.1 M Na_2SO_4 solution. Either the solution was preliminary purged with argon to remove dissolved oxygen (Fig. 4) or contained dissolved oxygen as a result of natural aeration (Fig. 5). The behavior of the Cu-Ni alloys in the sulfate solution depends on the nickel content in the alloy. The alloys with low nickel content (Cu7Ni, Cu30Ni) began to dissolve without passivation. The Cu50Ni and Cu70Ni alloys are passivated at 0.1–0.25 V.

The Cu-Ni alloys are characterized by markedly higher anodic currents compared to the borate buffer solution. the intense alloy dissolution in the aerated solution begins at slightly more negative potentials than in the solutions with dissolved oxygen. The anodic current peaks for Cu50Ni and Cu70Ni are considerably higher in the first solution than in the second one. For example, these currents with Cu50Ni are 2 and 0.3 mA/cm^2, respectively. An increase of the nickel content in the alloy leads to a decrease of the anodic currents over the whole potential range. The passivating effect of nickel in the Cu-Ni alloys was pointed out in previous studies [10–13].

The passivating effects of nickel and dissolved oxygen are markedly stronger in the sulfate solution than in the borate buffer solution. For example, it is seen from Figs. 1 and 4 that current peak A1 decreases by 1.4 times in the borate solution and by 7 times in the sulfate solution, when we pass from alloy Cu50Ni to alloy Cu70Ni.

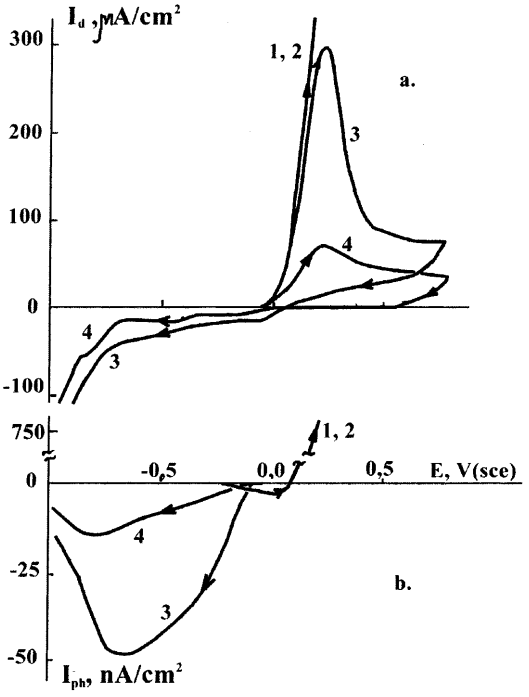

Fig. 5 **a** Dependence of dark current i_d and **b** corresponding dependence of photocurent i_{ph} (λ = 420 nm) on the potential for Cu-Ni alloys in the oxygen containing Na_2SO_4 solution (potential scan rate 2 mV/s)

For all studied alloys in the deaerated solution (the lower part of Fig. 4) the positive photocurrent begins to increase as soon as the dark anodic current starts to increase. Consequently, the anodic dissolution of Cu-Ni alloys occurs in the presence of photosensitive Cu_2O on the surface. This oxide is an n-type semiconductor, since the photocurrent is anodic. The photocurrents pass through a maximum.

The results obtained for Cu7Ni and Cu30Ni alloys are difficult to interprete because of the marked variations of the electrode surface owing to the intense dissolution.

As well as for the dark situation, the photocurrent is higher for the Cu50Ni alloy than for the Cu70Ni alloy. The photocurrent decays to zero as the potential increases. This occurs earlier for the Cu70Ni alloy than for Cu50Ni alloy. The amount of Cu_2O formed on the surface probably depends on the rate of alloy dissolution and, to a larger extent, on the nickel content of the alloy. The observed decrease of the photocurrent may be caused by the formation of a non-photosensitive oxide, CuO for example.

During the reverse scan from 0.8 to 0.0 V the photocurrents, as well as the dark currents, are hardly detectable. The absence of the dark current means that the passive film, which has formed at the potential of 0.8 V, is retained. The absence of the photocurrent means that the passive film consists of non-photosensitive oxides, e.g., from a mixture of NiO, CuO, oxides and $Cu(OH)_2$.

A shift to the more negative potentials for Cu50Ni and Cu70Ni alloys leads to the rise of negative photocurrents (p-type semiconductors), passing through a maximum. The appearance of the photocurrents means the formation of Cu_2O as a result of the reduction of passivating oxide. In this case, a dependence is observed inverse to that observed for the direct scan: the photocurrent for the Cu70Ni alloy is higher than for the Cu50Ni alloy. Probably, nickel promotes deeper alloy passivation and the accumulation of oxides, among them copper oxides, on the surface. Hence, high photocurrents are observed during the reduction. In the case of Cu50Ni alloy, the smaller amounts of copper oxides are retained on the surface, and, correspondingly, smaller Cu_2O photocurrents are recorded during reduction (a similar mechanism of nickel action may manifest itself in the behavior of the Cu7Ni and Cu30Ni alloys in the borate buffer).

For sulfate solution containing natural oxygen (Fig. 5), during the direct scan in the region of the onset of the small dark anodic current, a negative photocurrent is observed for the Cu7Ni and Cu30Ni alloys. After an abrupt increase of the dark current, which corresponds to the onset of activated dissolution, the photocurrent changes sign and may reach 750 nA/cm^2. The measurements were not conducted at the more positive potentials, because the electrode surface changed markedly owing to its dissolution. The initial negative photocurrent indicates the presence of the passive Cu_2O film, which is a p-type semiconductor. The film may thicken rapidly after activation, and the type of conductivity could change as a result of the variation of the oxide stoichiometry. Similar results were obtained using pure copper [24].

No photocurrent was detected using alloys high in nickel (50% and 70%) during the potential scan from −1.0 to 0.8 V. This may be associated with a change of alloy dissolution mechanism and the absence of Cu_2O on the electrode surface. No reverse scan was recorded for these reasons.

On the Cu50Ni and Cu70Ni alloys, no photocurrents are observed during the potential scan from 0.8 to 0.0 V. On these alloys the photocurrents appear at a potential somewhat more negative than the potential of the dark current appearance. The order of magnitude and the character of variation of the photocurrents differ little from those for the deaerated solution. However, the inverse dependence of the photocurrent peak on the nickel content of the alloy is important: the peak is higher for Cu50Ni alloy. However, no photocurrent decay to zero is observed even after the onset of hydrogen evolution, indicating that the oxide reduction is hampered. In this case, the presence of oxygen in the solution has a pronounced effect on the copper component and raises the degree of alloy passivation (lower dark currents). This favors the retention of copper oxides on the surface. The reduction of these oxides to Cu_2O yields the photocurrents proportional to the copper content of the alloy.

Spectral dependences of the photocurrent

The above photocurrent data were obtained using monochromatic illumination of specimens at a wavelength of 420 nm. To estimate the band gap of the anodic oxides, which had formed on the Cu-Ni alloys of various composition, we measured a wavelength dependence of the photocurrent.

The band gap was determined by the known equation [25]:

$$(i_{ph}) \cong \alpha \cong (hv - E_g)^n$$

where i_{ph} is the photocurrent, α is the absorption coefficient near the edge of proper absorption zone, hv is the photon energy, E_g is the band gap, and $n = 0.5$ and 2 for direct and indirect electron transitions, respectively. If we plot the equation using the coordinates $(i_{ph})^2$ versus hv and $(i_{ph})^{1/2}$ versus hv and extrapolate the dependencies to the abscissa, we find the band gap of the semiconductive oxide. Figure 6 gives the results obtained for the anodic oxide films on the Cu-Ni alloys of various composition. It is seen that the linear curve portions may be obtained both for $n = 0.5$ (direct transition) and $n = 2$ (indirect electron transition). In the first case the band gap is 2.6 ± 0.1 V; in the second case the band gap is 3.2 ± 0.1 V. According to the literature [3, 5, 24], the second value corresponds to Cu_2O. Consequently, for all systems studied (Cu-Ni alloys of various composition in the borate buffer solutions and sodium sulfate solutions), the band gap corresponds to Cu_2O only. The relatively low photocurrents due to other oxides, which may be present in the anodic film (mixed copper and nickel oxides, for example), are obscured by the high Cu_2O photocurrent.

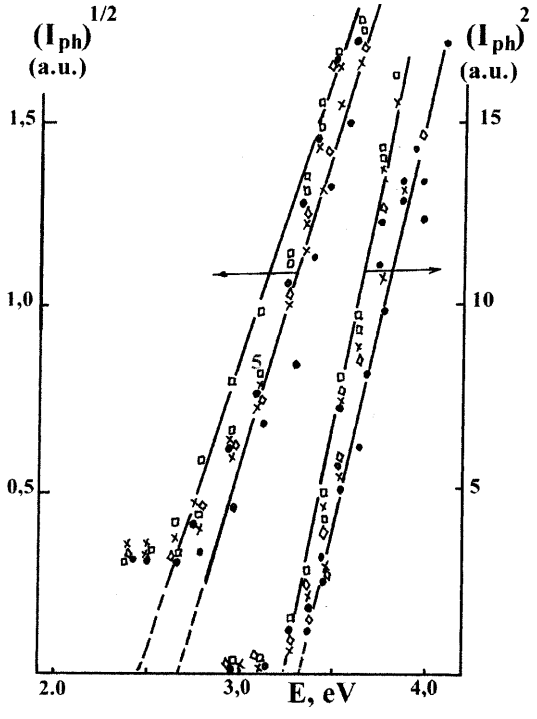

Fig. 6 $(i_{ph})^2$ vs. (hv) and $(i_{ph})^{1/2}$ vs. (hv) plots for alloys of various composition (● Cu7Ni, borate buffer; □ Cu7Ni, Na_2SO_4; × Cu30Ni, borate buffer; △ Cu50Ni, borate buffer; ◇ Cu50Ni, Na_2SO_4)

Conclusions

For copper, nickel, and several of their alloys in the borate buffer solution and 1 M Na_2SO_4 solution, the potentiodynamic polarization curves were measured from −0.8 to +0.8 V and the reverse curves were measured to −1.0 V. The corresponding photocurrent curves ($\lambda = 420$ nm) were obtained.

It is shown that the nickel content of the alloy has an effect on the anodic current and also on the current of the oxide cathodic reduction. Nickel in amounts of 7 and 30 wt% causes an increase of the anodic current. However, the larger amounts of nickel (50 and 70 wt%) lead to a decrease of the anodic current.

It is shown that oxygen dissolved in the electrolyte has a pronounced effect on the electrochemical behavior of the Cu-Ni alloys. The photocurrent measurements show that oxygen in the borate buffer solutions leads to the formation of passivating layers of p-type semiconductive Cu_2O. In the sulfate solution, the presence of oxygen leads to the formation of a passivating layer of Cu_2O, which is again a p-type semiconductor; this type changes at the potential of the onset of intense alloy dissolution.

Oxygen elimination from the boric-borate buffer solution leads to an increase of the anodic currents corresponding to the formation of p-type semiconductive oxides and alloy dissolution. Oxygen elimination from Na_2SO_4 solution leads to alloy dissolution and simultaneous formation of non-passivating Cu_2O that is an n-type semiconductor.

For all alloys in the potential ranges studied, the spectral dependences of the photocurrent show that the photosensitive oxides on the surface correspond to Cu_2O oxide with a band gap of 3.2 ± 0.1 eV.

References

1. Perez Sanchez M, Barrera M, Gonzalez S, Souto RM, Salvarezza RS, Arvia AJ (1990) Electrochim Acta 35: 1337
2. Souto RM, Gonzalez S, Salvarezza RS, Arvia AJ (1994) Electrochim Acta 39: 2619
3. Wilhelm SM, Tanizawa Y, Liu C-Y, Hackerman N (1982) Corros Sci 22: 791
4. Di Quarto F, Piazza S, Sunseri C (1985) Electrochim Acta 30: 315
5. Modestov AD, Guo-Ding Zhou, Hong-Hua Ge, Loo BH (1995) J Electroanal Chem 380: 63
6. Collisi U, Streblow H-H (1990) J Electroanal Chem 284: 385
7. Wilhelm SM, Hackerman N (1981) J Electrochem Soc 128: 1668
8. Dagan G, Wu-Mian Shen, Tamkiewicz M (1992) J Electrochem Soc 139: 1855

9. Sunseri C, Piazza S, Di Quarto F (1995) Mater Sci Forum 185–188: 435
10. Makhovetskaya IA, Scorchelletty VV (1966) Zashch Metalov 2: 617
11. Makhovetskaya IA, Scorchelletty VV (1967) Zashch Metalov 3: 161
12. Makhovetskaya IA, Scorchelletty VV, Odgiganova (1969) Zashch Metalov 5: 215
13. Makhovetskaya IA, Tochilkina RT (1970) J Appl Chem USSR 18: 1608
14. Kato C, Castle JE, Ateya BG, Pickering HW (1980) J Electrochem Soc 127: 1897
15. Mansfeld F, Lin G, Xiao X, Tsai CH, Little BY(1994) Corros Sci 36: 2063
16. Kato C, Pickering HW (1984) J Electrochem Soc 131: 1219
17. Lee HP, Ken Nobe (1984) J Electrochem Soc 131: 1236; (1993) J Electrochem Soc 140: 2483
18. Druska P, Strehblow H-H, Colledge S (1996) Corros Sci 38: 835
19. Druska P, Strehblow H-H (1995) Corros Sci 38: 1369
20. Hummel RE, Smith RJ (1988) Corros Sci 28: 279
21. Hummel RE, Smith RJ, Verink ED Jr (1987) Corros Sci 27: 803
22. Trabanelli G, Zucehi F, Brunoro G, Bologneri GP (1972) Thin Solid Films 13: 131
23. Bertocci U (1978) J Electrochem Soc 125: 1598
24. Kamkin A, Zhou Guoding, Xu Qunjie, Loo BH (1998) Trans Nonferrous Met Soc China 8: 304
25. Stimming U (1986) Electrochim Acta 31: 415